iScience

Article

Aberrant prefrontal activity and arousal level correlate with action initiation and response vigor in rats

Graphical abstract

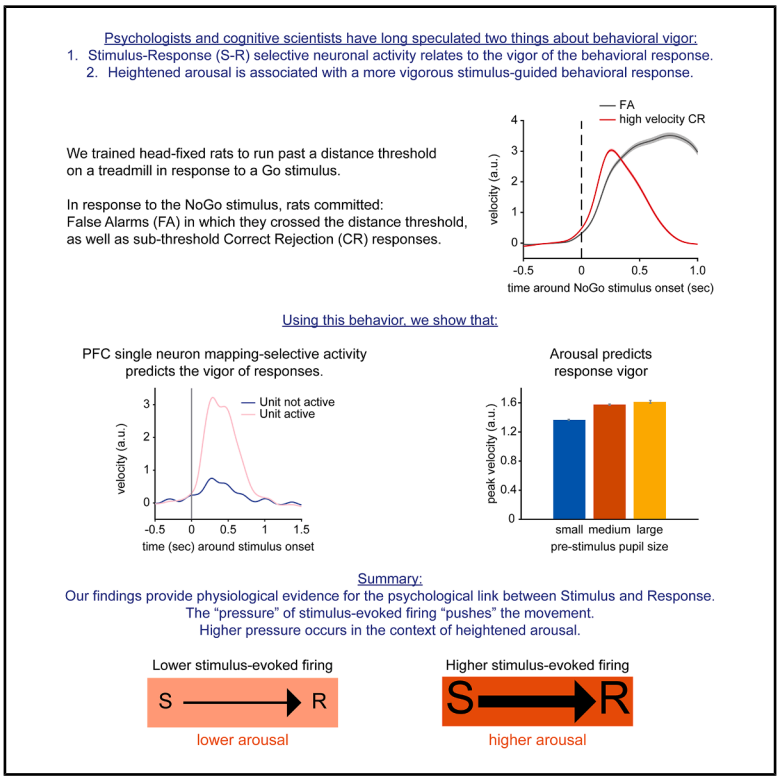

Highlights

- PFC single neuron stimulus-response (S-R) mapping activity relates to response vigor
- Activity is unrelated to temporal aspects of movement, but links the stimulus to the response
- S-R mapping activity ignites a behavioral Response which, however, can still be vetoed
- Heightened pre-stimulus arousal leads to higher Stimulus-guided Response vigor

Authors

Frederike J. Klein, Dmitrii Vasilev, Ryo Iwai, Masataka Watanabe, Nelson K. Totah

Correspondence

nelson.totah@helsinki.fi

In brief

Natural sciences; Biological sciences; Neuroscience; Systems neuroscience

Klein et al., 2026, iScience *29*, 115804
June 19, 2026
https://doi.org/10.1016/j.isci.2026.115804

CellPress

iScience

CellPress
OPEN ACCESS

Article

Aberrant prefrontal activity and arousal level correlate with action initiation and response vigor in rats

Frederike J. Klein,[1,2,3,6] Dmitrii Vasilev,[1,2,3,4,6] Ryo Iwai,[4] Masataka Watanabe,[4,5] and Nelson K. Totah[1,2,3,4,7,8,*]
[1]Helsinki Institute of Life Science (HiLIFE), University of Helsinki, 00014 Helsinki, Finland
[2]Faculty of Pharmacy, University of Helsinki, 00014 Helsinki, Finland
[3]Neuroscience Center, University of Helsinki, 00014 Helsinki, Finland
[4]Department of Physiology of Cognitive Processes, Max Planck Institute for Biological Cybernetics, 72076 Tübingen, Germany
[5]Department of Systems Innovation, School of Engineering, The University of Tokyo, Tokyo 113-8654, Japan
[6]These authors contributed equally
[7]Senior author
[8]Lead contact
*Correspondence: nelson.totah@helsinki.fi
https://doi.org/10.1016/j.isci.2026.115804

SUMMARY

Orchestrating learned stimulus-response (S-R) mappings is a central function of the prefrontal cortex (PFC), as evidenced by S-R selective neuronal activity during correct task performance. During errors, the "wrong" neurons are aberrantly activated. While movement vigor has been related to basal ganglia neural activity, the neural correlates linking S-R mappings to vigor remain elusive. We trained male rats to perform a head-fixed Go/NoGo task on a treadmill, enabling the recording of PFC single-unit spiking and running speed. Aberrant activation of the "wrong" S-R mapping predicts the initiation of incorrect responses, and the vigor of those responses scales with the strength of the aberrant stimulus-evoked activity. We show that such responses occur in the context of heightened arousal, addressing a classic but under-tested hypothesis linking arousal to vigor. These findings directly relate S-R mappings to response vigor and show how arousal is co-modulated with this relationship.

INTRODUCTION

The brain encounters a myriad of stimuli in any given moment. While not all these stimuli are used to control behavior, some of them are associated with specific responses. Think, for example, of a traffic light turning red and the potentially catastrophic consequences of failing to select the correct response: stopping. Stimulus-response (S-R) mappings, such as stopping at a red light, are often learned associations. Miller & Cohen[1] suggested that a primary function of the prefrontal cortex (PFC) is to represent learned S-R mappings and thus, select and initiate the appropriate stimulus-guided response. According to this theory, specific groups of PFC neurons should be activated after the presentation of a particular stimulus, S1, but only if the subject commits the correct stimulus-associated response (R1) and not when the subject makes the incorrect response (R2). Hence, these neurons represent the S1-R1 mapping.

In line with this hypothesis, when a stimulus-response (S-R) mapping is learned, subsets of PFC neurons in non-human primates become selectively responsive to specific stimuli.[2–8] Moreover, the stimulus-evoked activation of those neurons that acquire stimulus selectivity occurs only when the subject commits the response associated with that stimulus. Similar neuronal correlates of S-R mappings have been observed in the PFC of humans,[9,10] rodents,[11–14] and the nidopallium caudolaterale of corvids.[15–17]

Classically, the activity of S-R mapping selective PFC neurons has been described for trials in which the subject performed the correct response. Single neuron examples from error trials show that, in these trials, the "wrong" PFC neurons were aberrantly activated.[15–19] In other words, PFC neurons tuned to the S2-R2 mapping aberrantly responded after the presentation of the other stimulus, S1, and the subject subsequently committed an error (i.e., the response R2). We hypothesize that the strength of this aberrant activity and the "strength" or vigor of R2 are correlated.

While movement vigor has been directly related to the activity of striatum neurons,[20] the neural correlates of the vigor of a learned S-R mapping have remained elusive. Classic S-R mapping PFC studies[3,6,8,15–19,21] have made use of behavioral tasks in which the stimulus presentation and the subject's response are separated by a delay period. The mapping selective activity is observed during the delay period and is no longer apparent at the time of response initiation. This has made it impossible to relate the mapping selective activity to action initiation or the vigor of the subsequent response.

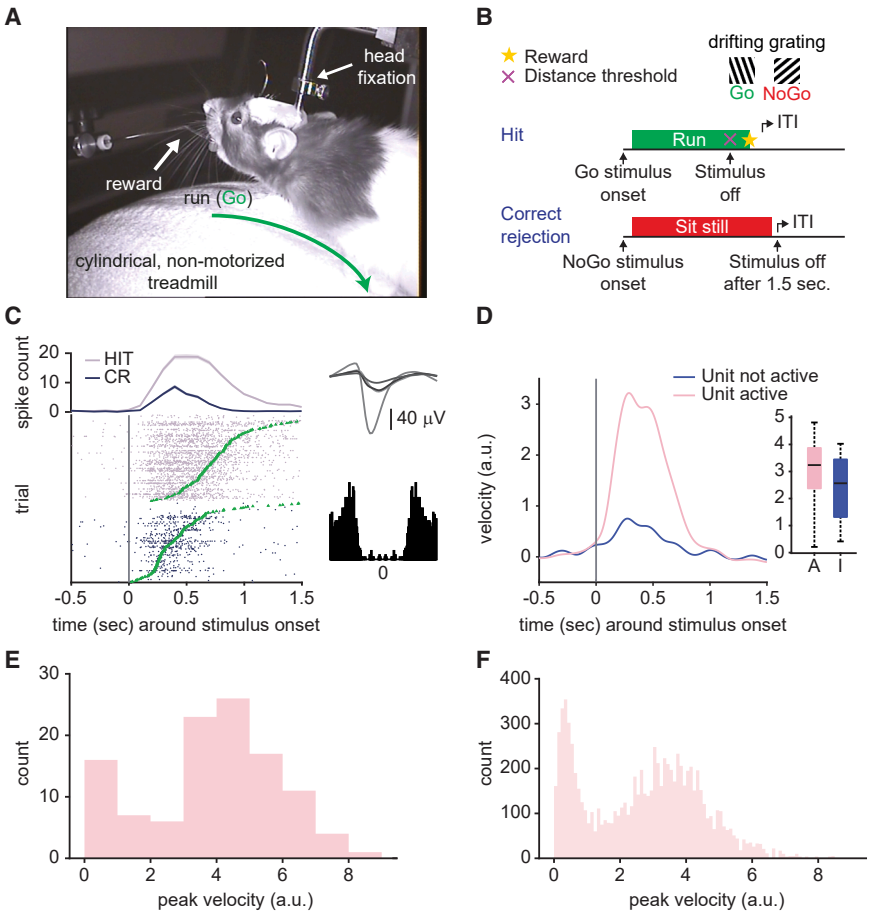

Figure 1. Activity of a Go stimulus-preferring unit and running behavior on CR trials

(A) Illustration of the set-up. Rats were head-fixed on a cylindrical, non-motorized treadmill. A reward spout was positioned in front of the rat's mouth through which 10% sucrose solution was delivered on Hit trials.

(B) A schematic shows trial progression for hit and correct rejection trials in the Go/NoGo task. The Go and NoGo stimuli consisted of a drifting grating with different orientations. Rats were required to sit immobile for at least 0.5 s prior to stimulus onset. In a Hit trial, the rat started running upon presentation of the Go stimulus until a distance threshold was crossed and reward was delivered. On trials in which the NoGo stimulus was presented, the rat was supposed to sit still until the stimulus was turned off for a successful CR response.

(C) Example single-unit spike raster plot (bottom left) and peri-stimulus time histogram (top left) for HIT and CR trials. The gray line marks the time of stimulus onset, and the green triangle marks the time at which peak velocity was reached. Trials were sorted by the time of peak velocity. Waveforms from the four channels with the strongest signal for this unit are shown on the right (top), as well as the autocorrelation for the example unit (bottom right).

(D) Velocity of the rat averaged across CR trials in which the example unit, shown in C, was active (pink) or not active (light blue). Trials in which the unit was active showed a brief period of running after the NoGo stimulus presentation. The inset shows, at the population level, the distribution of trial-averaged peak velocities for trials in which the units were active versus inactive (N = 56 units, excluding two of the Go stimulus-preferring units without active trials). The black line in the box plot shows the median and the whiskers show the range of the data. There were no outliers.

(E) A histogram of maximum velocity for each CR trial in which the example unit was active. This revealed a wide variability in peak velocities.

(F) A histogram shows peak velocity (same as in E), but for all CR trials across all 58 Go stimulus-preferring units.

Here, we investigate the relationship between the vigor or strength of a stimulus-guided response and the preceding mapping selective activity in the rat PFC. We find that the trial-specific strength of aberrant activity is directly correlated to incorrectly initiated running speed. We further demonstrate that a similar relationship can be observed for pre-stimulus pupil size and the running speed. These findings suggest that the extent to which a specific S-R mapping is activated in PFC can be directly related to the strength of the response that is initiated, and that response vigor in this context is modulated by pre-trial arousal state.

RESULTS

We recorded activity in the PFC of four male rats during a visually cued Go/NoGo task (Figures 1A and 1B). A total of 629 single units were recorded. 58 out of 629 units selectively responded to the Go stimulus in correctly performed trials. This means that they had a clear stimulus-evoked response in Hit trials, while they were not activated in correct rejection (CR) trials. Our analyses were focused on these 58 Go stimulus-preferring units, as they are responsive to one S-R mapping, Go stimulus (S1) – running (R1), and not responsive to the other mapping, NoGo stimulus (S2) – immobility (R2).

Activity in CR trials is correlated with incorrect action initiation

Despite Go-preferring units being primarily responsive in Hit trials relative to CR trials, the spike rasters made it apparent that individual Go stimulus-preferring units were also active in a subset of CR trials (see Figure 1C for one example unit). This aberrant activity appeared in trials in which the non-preferred (i.e., NoGo) stimulus was presented and in which the distance threshold for a false alarm was not crossed. We examined the response trajectory on trials with these aberrant activations. To do so, we averaged the post-stimulus velocity across these trials and compared to trials without activation (0 spikes during the 1 s window after stimulus onset). This analysis revealed that when the unit aberrantly activated, running was incorrectly initiated, but aborted before the rat crossed the distance threshold, thus avoiding a false alarm (Figure 1D). The evidence for a difference in velocity was extremely strong according to a Bayesian *t* test of

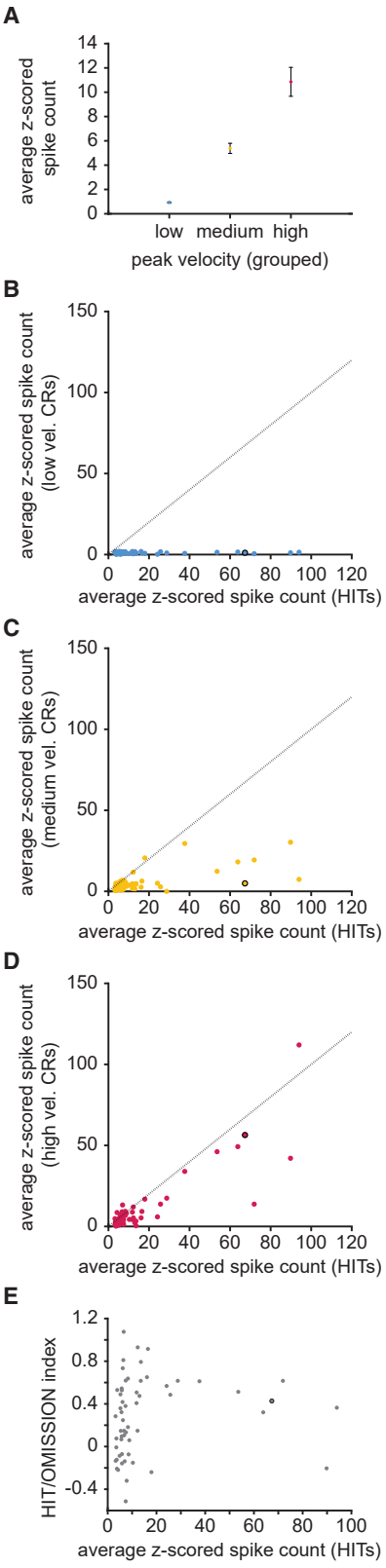

Figure 2. Relationship between peak velocity and stimulus-evoked spike counts

(A) Trials were grouped into sets with high, medium, and low peak velocity. Average z-scored spike count increased with peak velocity (N = 58 units). Error bars indicate the standard error of the mean. The low peak velocity group was different from both the medium (BF_{10} = 9689.83) and high (BF_{10} = 212.78) peak velocity groups. Evidence for a difference between the medium- and high-peak-velocity groups was only anecdotal (BF_{10} = 2.85).

(B) Z-scored spike count for HIT trials (x axis) and low peak velocity CR trials (y axis) for each of the 58 Go stimulus-preferring units. The example unit from Figures 2A–2C is marked with a gray circle.

(C) Same as B, but for medium peak velocity CR trials.

(D) Same as B, but for high peak velocity CR trials.

(E) Hit/Omission index values for all Go stimulus-preferring units plotted against z-scored Hit trial spike counts. Index values ≤ 0 indicate selectivity for the Go stimulus rather than selectivity for the S-R mapping.

the hypothesis that velocity was higher in trials when this example unit was active relative to inactive ($BF_{10} = 8.12 \times 10^4$). In order to assess this at the population level, we compared the peak of the velocity trace averaged across the trials when the unit was activated to the peak velocity averaged across trials in which the unit was not activated (Figure 1D, inset). Activation was defined, for each trial, as the NoGo stimulus-evoked firing rate exceeding a *Z* score of 2 over three consecutive 100 msec bins relative to a 500 msec pre-stimulus baseline. Two out of 58 units were excluded from the analysis due to an exceedingly low number of trials being compared in the active and inactive groups. We compared peak running velocity for active versus inactive trials at the population level (N = 56 units) using a Bayesian paired-samples one-sided *t* test of the hypothesis that velocity is greater when the units were active. We found strong support for this hypothesis (BF_{10} = 1745.23). This finding indicates that the activation of the aberrant S-R mapping is associated with the initiation of an incorrect response.

Strength of aberrant activity is correlated with response vigor

In the session in which this example unit was recorded, we observed that peak velocity varied across CR trials (Figure 1E). Since CR trials with aberrant activity were present across the population of 58 Go stimulus-preferring units, we assessed whether peak velocity varied at the level of the neuronal population. Similar to the example unit shown in Figures 1C–1E, trials in which the individual units were aberrantly active were accompanied by the incorrect initiation of motion with a variance in peak velocity (Figure 1F) before the animals stopped for an eventual CR. Since both the stimulus-evoked spike rate and peak velocity varied, we investigated whether the strength of activity was correlated with running speed (i.e., response vigor) on a trial-by-trial basis.

We investigated the relationship between the variability in neuronal activity and peak velocity on CR trials by splitting the trials into low, medium, and high peak velocity groups. As velocity increased, the NoGo stimulus-evoked activity across the 58 Go stimulus-preferring units increased (Figure 2A). A Bayesian repeated-measures ANOVA (N = 58 units) supported the alternative hypothesis of an activity difference depending on velocity (BF_{10} = 7816.95). Additionally, a traditional repeated-measures ANOVA yielded a *p*-value of <0.001 ($F_{2,2868}$ = 13.61). Bayesian post-hoc t-tests supported an obvious difference between low

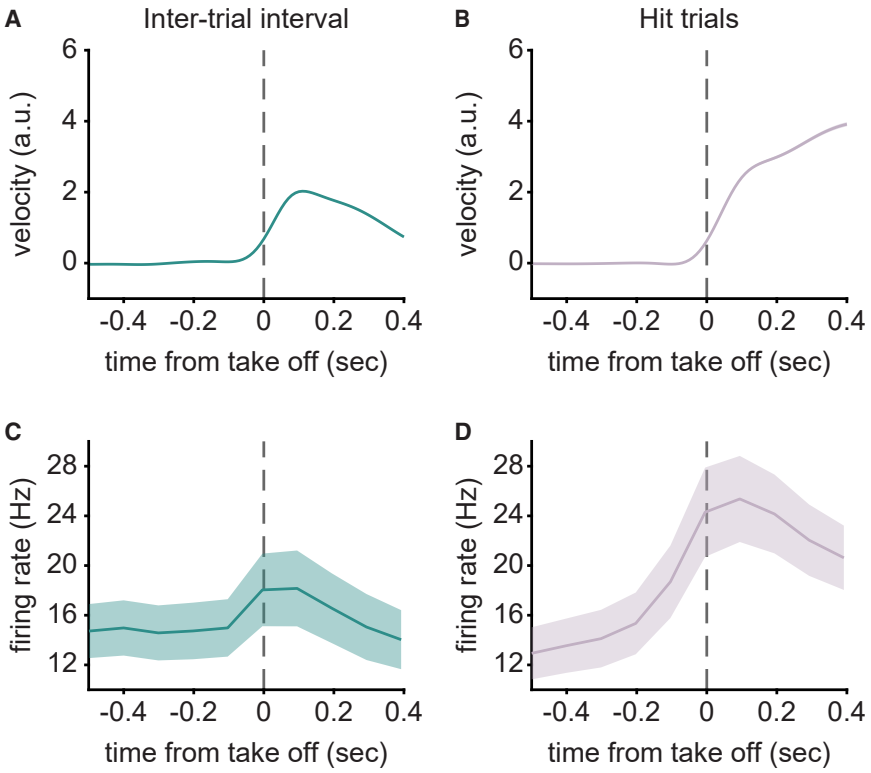

Figure 3. Running during Hit trials, not the ITI, modulates firing rate

(A) Episodes of ITI transitions from stationary to running (take-off) were selected. We found a total of 753 episodes for 47 of the 58 Go stimulus-preferring units. Running speed was averaged across those episodes, aligned to take-off. Shading represents two standard errors.

(B) Average running speed across all Hit trials aligned to take-off and plotted as in A.

(C) Average firing rate of 47 Go stimulus-preferring units aligned to take-off during the ITI. The firing rate has a minor modulation after take-off. A window of −0.4 to +0.5 s around take-off was chosen to ensure the window did not include parts of the previous or next trial. Shading represents two standard errors.

(D) Same as C, but for Hit trials. Firing rate increases strongly prior to and during take-off.

velocity compared to medium and high velocity trials (BF_{10} = 9689.83 and BF_{10} = 212.78, respectively, with corresponding *p*-values of <0.001 from traditional t-tests, respectively). The Bayesian analysis suggested that there is anecdotal evidence in favor of increased activity in high velocity trials compared to medium velocity trials (BF_{10} = 2.85) with a traditional *t* test yielding a *p*-value of 0.039. At the level of individual units (Figures 2B–2D), as response vigor increased, the activation gradually approached the level of activity on Hit trials. We quantified the similarity to Hit trials by calculating Pearson's correlation coefficient. Activity on low velocity CR trials was not significantly correlated with activity on Hit trials (r = 0.1199, *p* = 0.37). As response vigor increased, the correlation with Hit trial activity became significant and increasingly stronger (Hit vs. medium velocity CRs: r = 0.6451, *p* = 4.6087e−08; Hit vs. high velocity CRs: r = 0.8648, *p* = 2.1622e−18). Note that the increased activity with higher response vigor was most prominent for units with higher Hit trial spike count. The strength of the scaling may vary depending on factors such as electrode location in an anterior-posterior prefrontal gradient and/or cortical layer, both of which could vary across individual rats. In summary, the level of aberrant S-R mapping activity in PFC is directly related to the vigor with which the incorrect response is initiated in these trials.

While most of the Go stimulus-preferring units in our study responded on CR trials, when incorrect running was initiated, some units exhibited little to no increase in spike count. These units tended to fire at a lower rate on Hit trials. Thus, they might have only a slight preference for the Go stimulus, and given their low activity level, scaling with response velocity could be difficult to observe. On the other hand, it is possible that these units do not represent the S-R mapping but rather developed a preference for the Go stimulus itself. In this case, we would not expect any scaling and instead expect the units to remain unresponsive to the NoGo stimulus. To test this, we computed a Hit/Omission index (see Methods). If a unit is selective for the Go stimulus itself rather than the S-R mapping, then it should also be active in Omission trials since the same stimulus is presented. If a unit is not encoding the S-R mapping, then the index will be close to 0 or negative. For S-R mapping selective units, we expect a higher index value since these units should not be active in Omission trials (when no response is initiated). We indeed observed a group of units with negative Hit/Omission index values, which were almost exclusively those with low Hit trial spike counts (Figure 2E). Therefore, we can assume that a subset of the Go stimulus-preferring units is purely selective for the Go stimulus itself rather than the mapping of this stimulus to running. This explains the lack of response scaling with running speed in CR trials for those units.

Finally, it is possible that this neuronal activity does not link response vigor to an S-R mapping, but is rather neuronal activity simply related to the initiation of running itself. For instance, in both CR trials and Hit trials, an example neuron (Figure 1C) supposedly encoding an S-R mapping gradually increases its firing after stimulus onset until peak velocity is reached (marked by a green triangle in Figure 1C). It is possible that this unit is simply responding during take-offs (i.e., transitions from stationary to running) outside the S-R context. We tested whether this was the case for all putative S-R encoding single units by selecting times from the inter-trial interval (ITI) in which the rats were initially immobile but subsequently started to run (Figure 3A). We found a total of 753 such events. While the peak velocity reached was lower than in Hit trials and the duration of running was shorter during the ITI, the characteristic steep increase of

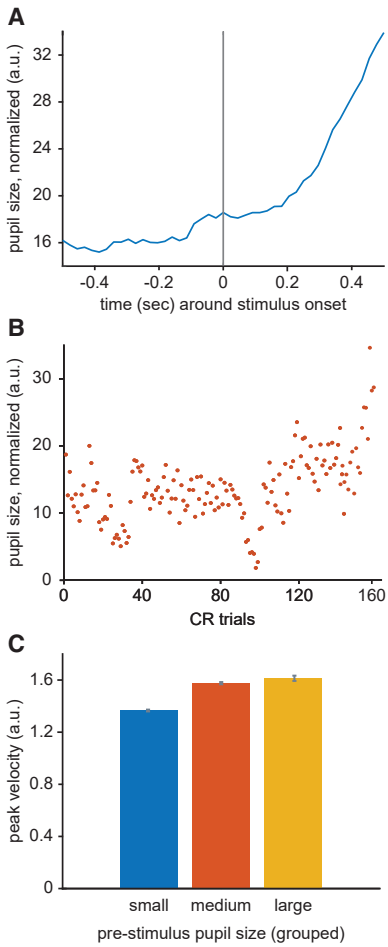

Figure 4. Pre-stimulus pupil size is related to peak velocity

(A) One example of the pupil size trace around the time of stimulus onset.

(B) Averaged pre-stimulus pupil size (0.5 s before stimulus onset until stimulus onset) across trials (one session from one rat).

(C) Trials are grouped into sets with large, medium, and small pre-stimulus pupil size. This was done by taking the maximum and minimum pupil size per session and subsequently splitting this range into tertiles. We analyzed 183,777 trials in total from 37 rats. The peak velocity was different for small versus medium ($BF_{10} = 1.27\times10^{74}$) and small versus large ($BF_{10} = 4.98\times10^{27}$) pre-stimulus pupil size groups. There was no evidence for a difference in peak velocity between the medium and large pupil size groups ($BF_{10} = 0.08$). Error bars indicate the standard error of the mean.

velocity could be observed in both conditions (Figure 3A versus Figure 3B). We aligned the activity of the 47 Go stimulus-preferring units (the subset of units for which ITI take-offs could be identified) to the time of take-off for both Hit trial running and ITI running. The analysis window was shorter (−0.5 to +0.4 s around take-off) to ensure that the window did not include parts of the previous or next trial in the ITI case. If S-R mapping units are actually encoding the vigor of responses in general, then the activity should increase after take-offs during the ITI and in Hit trials. On the other hand, the S-R mapping units should only increase activity during Hit trials. We found that, in Hit trials, activity peaked during the increase of velocity, as expected (Figure 3D). However, during the ITI, firing rate changed only minimally (Figure 3C). A Bayesian 2-way repeated-measures ANOVA suggested that these data are strong evidence for the change in firing rate over time, differing between ITI and Hit take-offs ($BF_{10} = 5.230\times10^{47}$). Therefore, the neuronal activity is not related to running speed itself, but only related to running speed in the context of Go stimulus presentation. Activity in Hit trials and aberrant activity in CR trials both appear to link stimulus onset to the peak of the behavioral response. The Go stimulus-preferring units thus represent the S-R mapping and not running initiation, per se.

Pre-stimulus arousal is related to peak velocity

One factor that has been shown to influence response speed or reaction time and thus response vigor is arousal. We used a dataset including pupillometry data from 37 rats performing the same Go/NoGo task. Pupil size is a proxy for the arousal state.[22] We focused on pupil size in a 0.5 s window prior to stimulus presentation in CR trials (see Figure 4A for an example). Pupil size was then averaged across this time window. This revealed variable pupil sizes across the duration of a single recording session (Figure 4B). We tested whether pre-stimulus pupil size was correlated with the vigor of incorrectly initiated responses by splitting the trials into three groups based on pupil size (small, medium, and large pupils). Peak velocity for small pupil trials was significantly slower than for the other two pupil size conditions (Figure 4C). Both Bayesian independent samples ANOVA supported an effect of pre-stimulus pupil size on response velocity ($BF_{10} = 6.37\times10^{85}$), which was due to slower response velocities when pre-stimulus pupil size was small (post-hoc Bayesian *t* test, $BF_{10} = 1.27\times10^{74}$ and $BF_{10} = 4.98\times10^{27}$ for small versus medium and large pupil sizes, respectively). A post-hoc Bayesian *t* test comparing velocity for medium and large pre-stimulus pupil sizes provided strong evidence in support of the null hypothesis that velocity did not differ ($BF_{10} = 0.08$), which was in line with a traditional *t* test ($T = -1.70$, $p = 0.205$). Given that velocity distributions are truncated at 0 (and are thus not normal distributions), we also conducted a classical Kruskal-Wallis Test followed by post-hoc Dunn's tests on log-transformed data and the results agreed with the Bayesian statistics ($H = 494.74$, $p < 0.001$; low versus medium: $Z = -20.57$, Bonferroni corrected *p*-value <0.001; low versus high: $Z = -12.64$, Bonferroni corrected *p*-value <0.001; medium versus high: $Z = -1.70$, Bonferroni corrected *p*-value = 0.266). This pupil-vigor relationship resembles the relationship between aberrant neuronal activity and peak velocity. Therefore, increased arousal may modulate vigor by making aberrant S-R mapping activations more likely.

Aberrant PFC activity contributes to an ignition process

Our results align with previous findings in support of the Global Neuronal Workspace (GNW) theory.[23,24] According to this theory, conscious report of a stimulus requires that a state of "ignition" is reached in the frontal cortex. This ignition state is a strong, transient increase in activity around 300 msec post stimulus. A recent study has shown that in the context of a detection task, ignition can be reached sometimes in stimulus-absent trials due to fluctuating activity in PFC.[25] On these trials, the subject commits a false alarm. The PFC activity we observed also peaks

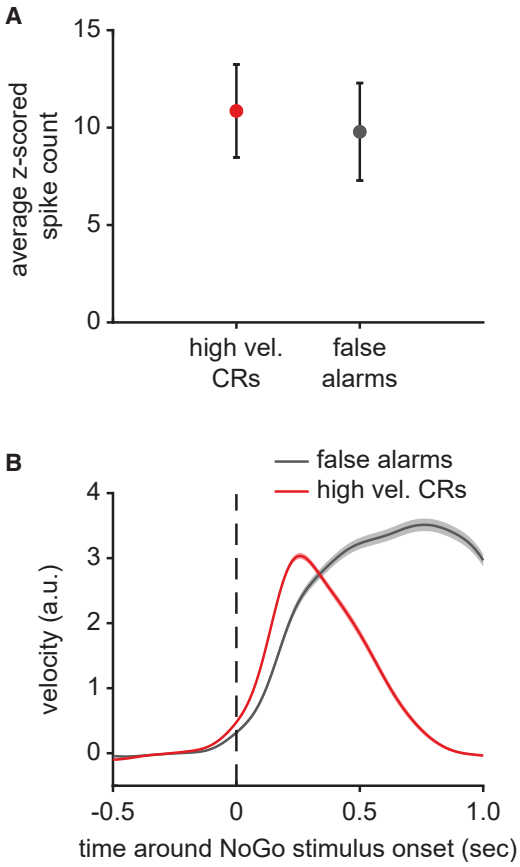

Figure 5. False alarm and high-velocity CR trials are both associated with aberrant activity

(A) Average z-scored spike count for high velocity CR trials and false alarm trials (N = 58 units). A Bayesian paired *t* test revealed moderate-to-strong evidence for no difference in activity between CR trials and false alarm trials (BF_{10} = 0.162). Error bars indicate the standard error of the mean.

(B) Average velocity profile for high velocity CR trials and false alarm trials were roughly matched until the response was vetoed in the high velocity CR trials. Shading indicated standard error of the mean.

around 300 msec post-stimulus and is followed by response initiation. The aberrant S-R mapping activity could thus be considered an example of the wrong "pool" of neurons reaching the state of ignition and driving an overt (but incorrect) behavioral response. If aberrant activation of Go stimulus-preferring neurons is a state of ignition that drives an incorrect response, then, as the level of aberrant activation to the NoGo stimulus approaches the level that those neurons typically exhibit on Hit trials, the rat should commit a false alarm. In line with this prediction, the stimulus-evoked activity during false alarm trials was significantly correlated with Hit trial activity (r = 0.7241, *p* = 1.9553e−10). These results indicate that the aberrant activity of the Go stimulus-preferring units contributes to the ignition of the incorrect response in trials in which the NoGo stimulus is presented.

GNW theory would predict that reaching ignition would mandate a false alarm. However, we observe aberrant activations that do not lead to false alarms, but instead subthreshold responses on CR trials. Given that we observed a linear relationship between aberrant activity level and the vigor of subthreshold responses, false alarm trials should be associated with the most extreme aberrant activation level and the highest response vigor. In contrast to this prediction, we found that the aberrant activity was similar in high velocity CR trials and false alarm trials (Figure 5A). A Bayesian paired *t* test indicated that these data are moderate-to-strong evidence for no difference in activity between CR trials and false alarm trials (BF_{10} = 0.162). Peak response vigor on these CR trials was roughly matched to the vigor on false alarm trials (Figure 5B), with the only difference being that the in-progress false alarm response was vetoed on the CR trials. This result suggests that reaching ignition mandates a high vigor behavioral response, but this response can, in some cases, be vetoed.

DISCUSSION

A primary function of the PFC is to represent learned S-R mappings, and thus, the PFC is thought to select and initiate the appropriate stimulus-guided response.[1] While behavioral response vigor has been directly related to the activity of striatum neurons,[20] the neural correlates of the vigor of a learned S-R mapping have remained elusive. In this study, we investigated how the activity of S-R mapping encoding units in the PFC of rats relates to response initiation and response vigor. We show that when one S-R mapping is activated, in the presence of the other stimulus, the incorrect response is initiated. The vigor of this incorrect response is correlated with the strength of PFC neuronal activation. While both the Hit trial activity and the CR trial aberrant activity link stimulus onset to peak velocity by ramping up, this activity is not related to the initiation of running itself. In the ITI, where no stimulus is present, Go stimulus-preferring units did not increase their activity as rats took off from a stationary to a running state. Our finding is akin to the "pressure" of stimulus-evoked firing, "pushing" the movement. Critically, however, we show that the neuronal spiking is not related to the temporal aspects of the movement, per se, but instead "links" or "bridges" the S to the R.

If this neuronal activity is indeed a cognitive link to the R and contributes to response vigor, then it might be assumed that the activation strength of Go-stimulus preferring units is related to response vigor on Hit trials. In these trials, the correct S-R mapping is activated, and the rat responds by running (in the presence of the Go stimulus) until it crosses the distance threshold and obtains a reward. The trial-by-trial activation strength of this S-R mapping may correlate with the response vigor (velocity). This potential scenario cannot be tested in this behavioral task because Hit trial responses have a stereotyped velocity profile characterized by an increase in velocity followed by a lasting plateau of steady running speed that is similar across trials. There is no clearly discriminable peak in velocity, nor are there different plateau speeds. Thus, grouping trials into different levels of response vigor is impossible in this task (and the same applies to false alarm trials). Nevertheless, it remains possible that Go stimulus-preferring units contribute to response vigor in all trial types.

One might wonder if this framework extends to all task stimuli, such as the NoGo stimulus. The response vigor might also be

related to the activation strength of NoGo stimulus-preferring neurons linked with the other R (i.e., sitting still). We could not test this possibility in this dataset because none of the units were NoGo stimulus-preferring. Single units in this subregion are known to be selective exclusively for reward-associated stimuli.[14,26] In our paradigm, only the Go stimulus is associated with the possibility of reward. This likely explains why we did not observe units with a preference for the unrewarded NoGo stimulus.

The link between S-R mapping encoding and the vigor of the subsequent response is completely dependent on the learned context of this task. By analogy, humans have learned to stop in response to red traffic lights, but not all red lights. It is important to note that our findings do not suggest that PFC stimulus-evoked neuronal activity will necessitate or evoke running outside of the task context used here. In a confined context with specific response requirements, S-R mappings are an efficient representation of the task demands. Thus, S-R mappings are a building block for the variety of cases where PFC neurons become selective to task parameters, such as abstract rules,[8,11,15,27] a stimulus (or stimulus feature) itself,[7,21,28] motor preparation,[18] or the value of a stimulus.[14]

Classic S-R mapping PFC studies[3,6,8,15–19,21] have made use of behavioral tasks in which the stimulus presentation and the subject's response are separated by a delay period. The mapping selective activity is observed during the delay period and is no longer apparent at the time of response initiation. This has made it impossible to relate the mapping selective activity to action initiation or the vigor of the subsequent response. Here, we were able to connect response vigor with the strength of preceding mapping selective activity by continuous measurement of running speed.

We furthermore show that pre-stimulus arousal is related to the vigor of these incorrectly initiated responses. Heightened arousal has been associated with committing errors and shown to modulate anterior cingulate cortex activity.[29] Arousal and task performance have an inverted-U-shaped relationship, whereby hypoarousal and hyperarousal are associated with poorer task performance compared to intermediate arousal levels.[30,31] Our data show a linear relationship between arousal and response vigor instead. This linear relationship might directly relate to the inverted-U relationship for performance: In states of low arousal, response vigor is weak to the extent that responses might not even be initiated, which leads to an increased number of omissions (i.e., poorer performance). With increasing arousal response, vigor increases, which leads to a higher number of Hits and initiated incorrect responses that can still be aborted (as demonstrated by the subthreshold response reported here in a subset of CR trials). A high number of Hits and CRs is considered optimal task performance. Once arousal exceeds this optimal level and responses continue increasing in vigor, it will be harder to stop already initiated incorrect responses prior to response threshold crossing. Therefore, the number of false alarms will increase, and performance will drop. The linear relationship between arousal and response vigor might partially explain the commonly observed inverted-U-shaped relationship between arousal and task performance.

Given that arousal-related brain regions, such as the locus coeruleus, project to the PFC in rats (and non-human primates),[32,33] our results suggest the possibility that arousal and neuromodulation of the PFC could promote aberrant S-R mapping activity and thus the initiation or "ignition" of incorrect responses (hence the association to error trials) and the vigor of those responses. It has long been postulated that arousal systems are linked to response vigor,[34] but this link has not been thoroughly tested until recently.[35] Our results further support this link and, moreover, suggest a possible neuronal mechanism for the arousal-vigor relationship. Increased neuromodulatory system activity may bias PFC neuronal activity toward increased S-R mapping encoding activity, which in turn would drive higher response vigor for the subsequent behavioral response.

Our results expand GNW theory in two new directions. First, we show that the intensity of ignition could be directly linked to the vigor of the subsequent response. Second, the fact that the response in our paradigm was aborted before the animals committed an error suggests that behaviors triggered by a state of ignition can still be stopped. This behavior most likely requires a second conscious decision to follow the first one very quickly. GNW theory predicts that this second conscious decision requires a second ignition state. In our task context, this would be akin to the internally driven activation of the "correct pool" of S-R mapping selective neurons. The failure to reach this second ignition would allow the subthreshold response to continue past the threshold and thus produce a false alarm. In line with this interpretation, we observe similar initial velocity profiles for false alarm trials and the subset of CR trials with the highest velocity subthreshold responses. The first ignition is sufficient to trigger the initiation of a response. If that response is aborted prior to threshold crossing or fully executed as a false alarm may be determined by whether or not the second S-R mapping representation reaches ignition. The two expansions of the GNW theory proposed here indicate the need to investigate the interplay of different conscious decisions and, hence, the interplay of different states of ignition, as well as the relationship between ignition states and response vigor.

Limitations of the study

Our study supports a relationship between S-R mapping, associated neuronal activity, and response vigor. However, this was only demonstrated for Go stimulus-preferring neurons. This is likely due to the asymmetric rewarding of only hit responses in this task, given that neurons at the recorded location preferentially respond to rewarded stimuli. Therefore, while we speculate that the vetoing of the sub-threshold Go response may be preceded by a late activation of NoGo stimulus-preferring neurons, this remains to be demonstrated in rats performing a version of the task with symmetrical reward (i.e., rewarded CR trials). While our results suggest that the relationship between S-R mapping, associated neuronal activity, and response vigor may occur in the context of increasing arousal, the PFC neuronal activity recordings and pupillometry were not recorded simultaneously.

RESOURCE AVAILABILITY

Lead contact

Requests for further information and resources should be directed to and will be fulfilled by the lead contact, Nelson K. Totah (nelson.totah@helsinki.fi).

Materials availability

This study did not generate new unique reagents.

Data and code availability

- Behavior, treadmill velocity, pupillometry, single unit spiking data, and code used to perform the analyses and visualize the results have been deposited at https://etsin.fairdata.fi/ and are publicly available as of the date of publication. Etsin Data: https://doi.org/10.23729/fd-fde5397b-d01f-368a-9be1-a750d5f4d589.
- Any additional information required to reanalyze the data reported in this paper is available from the lead contact upon request.

ACKNOWLEDGMENTS

This work was funded by the University of Helsinki (Helsinki Institute of Life Science), the Sigrid Jusélius Foundation, the Research Council of Finland (Project Grant, decision 358106), and the Max Planck Society.

AUTHOR CONTRIBUTIONS

Conceptualization – F.J.K. and N.K.T.; data curation – D.V.; formal analysis – D.V. and F.J.K.; funding acquisition – N.K.T.; investigation – D.V. and R.I.; methodology – N.K.T. and M.W.; software – D.V.; supervision – N.K.T.; visualization – F.J.K. and D.V.; writing – original draft – F.J.K. and D.V.; writing – review and editing – F.J.K., D.V., M.W., and N.K.T.

DECLARATION OF INTERESTS

The authors declare no competing financial interests.

DECLARATION OF GENERATIVE AI AND AI-ASSISTED TECHNOLOGIES IN THE WRITING PROCESS

During the preparation of this work, the authors did not use an AI tools.

STAR★METHODS

Detailed methods are provided in the online version of this paper and include the following:

- KEY RESOURCES TABLE
- EXPERIMENTAL MODEL AND STUDY PARTICIPANT DETAILS
- METHOD DETAILS
  - Surgery
  - Handling and water restriction
  - Head-fixation and behavioral apparatus
  - Habituation to head-fixation and behavioral task training
  - Neurophysiological recordings and spike sorting
- QUANTIFICATION AND STATISTICAL ANALYSIS
  - Single unit spike count analysis
  - ITI analysis
  - Pupil analysis
  - Statistics

Received: April 28, 2025
Revised: November 1, 2025
Accepted: April 15, 2026
Published: April 20, 2026

REFERENCES

1. Miller, E.K., and Cohen, J.D. (2001). AN INTEGRATIVE THEORY OF PREFRONTAL CORTEX FUNCTION. Annu. Rev. Neurosci. *24*, 167–202. https://doi.org/10.1146/annurev.neuro.24.1.167.
2. Yamatani, K., Ono, T., Nishijo, H., and Takaku, A. (1990). Activity and Distribution of Learning-Related Neurons in Monkey (Macaca fuscata) Prefrontal Cortex. Behav. Neurosci. *104*, 503–531. https://doi.org/10.1037/0735-7044.104.4.503.
3. Sakagami, M., and Niki, H. (1994). Encoding of behavioral significance of visual stimuli by primate prefrontal neurons: relation to relevant task conditions. Exp. Brain Res. *97*, 423–436. https://doi.org/10.1007/bf00241536.
4. Miller, E.K., Erickson, C.A., and Desimone, R. (1996). Neural Mechanisms of Visual Working Memory in Prefrontal Cortex of the Macaque. J. Neurosci. *16*, 5154–5167. https://doi.org/10.1523/jneurosci.16-16-05154.1996.
5. Niki, H. (1974). Prefrontal unit activity during delayed alternation in the monkey. II. Relation to absolute versus relative direction of response. Brain Res. *68*, 197–204. https://doi.org/10.1016/0006-8993(74)90389-8.
6. Watanabe, M. (1986). Prefrontal unit activity during delayed conditional Go/No-go discrimination in the monkey. I. Relation to the stimulus. Brain Res. *382*, 1–14. https://doi.org/10.1016/0006-8993(86)90104-6.
7. Bichot, N.P., Schall, J.D., and Thompson, K.G. (1996). Visual feature selectivity in frontal eye fields induced by experience in mature macaques. Nature *381*, 697–699. https://doi.org/10.1038/381697a0.
8. Sakagami, M., and Tsutsui, K. (1999). The hierarchical organization of decision making in the primate prefrontal cortex. Neurosci. Res. *34*, 79–89. https://doi.org/10.1016/s0168-0102(99)00038-3.
9. Woolgar, A., Hampshire, A., Thompson, R., and Duncan, J. (2011). Adaptive Coding of Task-Relevant Information in Human Frontoparietal Cortex. J. Neurosci. *31*, 14592–14599. https://doi.org/10.1523/jneurosci.2616-11.2011.
10. Woolgar, A., Thompson, R., Bor, D., and Duncan, J. (2011). Multi-voxel coding of stimuli, rules, and responses in human frontoparietal cortex. Neuroimage *56*, 744–752. https://doi.org/10.1016/j.neuroimage.2010.04.035.
11. Reinert, S., Hübener, M., Bonhoeffer, T., and Goltstein, P.M. (2021). Mouse prefrontal cortex represents learned rules for categorization. Nature *593*, 411–417. https://doi.org/10.1038/s41586-021-03452-z.
12. Peters, Y.M., O'Donnell, P., and Carelli, R.M. (2005). Prefrontal cortical cell firing during maintenance, extinction, and reinstatement of goal-directed behavior for natural reward. Synapse *56*, 74–83. https://doi.org/10.1002/syn.20129.
13. Schoenbaum, G., and Eichenbaum, H. (1995). Information coding in the rodent prefrontal cortex. I. Single-neuron activity in orbitofrontal cortex compared with that in pyriform cortex. J. Neurophysiol. *74*, 733–750. https://doi.org/10.1152/jn.1995.74.2.733.
14. Wal, A., Klein, F.J., Born, G., Busse, L., and Katzner, S. (2021). Evaluating Visual Cues Modulates Their Representation in Mouse Visual and Cingulate Cortex. J. Neurosci. *41*, 3531–3544. https://doi.org/10.1523/jneurosci.1828-20.2021.
15. Veit, L., and Nieder, A. (2013). Abstract rule neurons in the endbrain support intelligent behaviour in corvid songbirds. Nat. Commun. *4*, 2878. https://doi.org/10.1038/ncomms3878.
16. Veit, L., Pidpruzhnykova, G., and Nieder, A. (2015). Associative learning rapidly establishes neuronal representations of upcoming behavioral choices in crows. Proc. Natl. Acad. Sci. *112*, 15208–15213. https://doi.org/10.1073/pnas.1509760112.
17. Moll, F.W., and Nieder, A. (2015). Cross-Modal Associative Mnemonic Signals in Crow Endbrain Neurons. Curr. Biol. *25*, 2196–2201. https://doi.org/10.1016/j.cub.2015.07.013.
18. Chen, T.-W., Li, N., Daie, K., and Svoboda, K. (2017). A Map of Anticipatory Activity in Mouse Motor Cortex. Neuron *94*, 866–879.e4. https://doi.org/10.1016/j.neuron.2017.05.005.
19. Schmitt, L.I., Wimmer, R.D., Nakajima, M., Happ, M., Mofakham, S., and Halassa, M.M. (2017). Thalamic amplification of cortical connectivity sustains attentional control. Nature *545*, 219–223. https://doi.org/10.1038/nature22073.
20. Panigrahi, B., Martin, K.A., Li, Y., Graves, A.R., Vollmer, A., Olson, L., Mensh, B.D., Karpova, A.Y., and Dudman, J.T. (2015). Dopamine Is

Required for the Neural Representation and Control of Movement Vigor. Cell *162*, 1418–1430. https://doi.org/10.1016/j.cell.2015.08.014.

21. Sakagami, M., and Niki, H. (1994). Spatial selectivity of go/no-go neurons in monkey prefrontal cortex. Exp. Brain Res. *100*, 165–169. https://doi.org/10.1007/bf00227290.
22. Bradshaw, J. (1967). Pupil Size as a Measure of Arousal during Information Processing. Nature *216*, 515–516. https://doi.org/10.1038/216515a0.
23. Dehaene, S., Kerszberg, M., and Changeux, J.-P. (1998). A neuronal model of a global workspace in effortful cognitive tasks. Proc. Natl. Acad. Sci. *95*, 14529–14534. https://doi.org/10.1073/pnas.95.24.14529.
24. Mashour, G.A., Roelfsema, P., Changeux, J.-P., and Dehaene, S. (2020). Conscious Processing and the Global Neuronal Workspace Hypothesis. Neuron *105*, 776–798. https://doi.org/10.1016/j.neuron.2020.01.026.
25. van Vugt, B., Dagnino, B., Vartak, D., Safaai, H., Panzeri, S., Dehaene, S., and Roelfsema, P.R. (2018). The threshold for conscious report: Signal loss and response bias in visual and frontal cortex. Science *360*, 537–542. https://doi.org/10.1126/science.aar7186.
26. Jendryka, M.M., Lewin, U., Kapanaiah, S.K.T., Dermutz, H., Liss, B., Pekcec, A., Akam, T., Grewe, B.F., and Kätzel, D. (2024). Excitatory neurons of the anterior cingulate cortex encode chosen actions and their outcomes rather than cognitive state. Preprint at bioRxiv. https://doi.org/10.1101/2024.04.12.589244.
27. Wallis, J.D., Anderson, K.C., and Miller, E.K. (2001). Single neurons in prefrontal cortex encode abstract rules. Nature *411*, 953–956. https://doi.org/10.1038/35082081.
28. Lauwereyns, J., Sakagami, M., Tsutsui, K., Kobayashi, S., Koizumi, M., and Hikosaka, O. (2001). Responses to Task-Irrelevant Visual Features by Primate Prefrontal Neurons. J. Neurophysiol. *86*, 2001–2010. https://doi.org/10.1152/jn.2001.86.4.2001.
29. Ebitz, R.B., and Platt, M.L. (2015). Neuronal Activity in Primate Dorsal Anterior Cingulate Cortex Signals Task Conflict and Predicts Adjustments in Pupil-Linked Arousal. Neuron *85*, 628–640. https://doi.org/10.1016/j.neuron.2014.12.053.
30. de Gee, J.W., Mridha, Z., Hudson, M., Shi, Y., Ramsaywak, H., Smith, S., Karediya, N., Thompson, M., Jaspe, K., Jiang, H., et al. (2024). Strategic stabilization of arousal boosts sustained attention. Curr. Biol. *34*, 4114–4128.e6. https://doi.org/10.1016/j.cub.2024.07.070.
31. Arnsten, A.F.T., Wang, M.J., and Paspalas, C.D. (2012). Neuromodulation of Thought: Flexibilities and Vulnerabilities in Prefrontal Cortical Network Synapses. Neuron *76*, 223–239. https://doi.org/10.1016/j.neuron.2012.08.038.
32. Chandler, D.J., Gao, W.-J., and Waterhouse, B.D. (2014). Heterogeneous organization of the locus coeruleus projections to prefrontal and motor cortices. Proc. Natl. Acad. Sci. *111*, 6816–6821. https://doi.org/10.1073/pnas.1320827111.
33. Levitt, P., Rakic, P., and Goldman-Rakic, P. (1984). Region-specific distribution of catecholamine afferents in primate cerebral cortex: A fluorescence histochemical analysis. J. Comp. Neurol. *227*, 23–36. https://doi.org/10.1002/cne.902270105.
34. Nieuwenhuis, S. (2024). Arousal and performance: revisiting the famous inverted-U-shaped curve. Trends Cognit. Sci. *28*, 394–396. https://doi.org/10.1016/j.tics.2024.03.011.
35. Beerendonk, L., Mejías, J.F., Nuiten, S.A., Gee, J.W. de, Fahrenfort, J.J., and Gaal, S. van (2024). A disinhibitory circuit mechanism explains a general principle of peak performance during mid-level arousal. Proc. Natl. Acad. Sci. *121*, e2312898121. https://doi.org/10.1073/pnas.2312898121.
36. Pachitariu, M., Sridhar, S., Pennington, J., and Stringer, C. (2024). Spike sorting with Kilosort4. Nat. Methods *21*, 914–921. https://doi.org/10.1038/s41592-024-02232-7.
37. Vasilev, D., Raposo, I., and Totah, N.K. (2023). Brightness illusions evoke pupil constriction preceded by a primary visual cortex response in rats. Cerebr. Cortex *33*, 7952–7959. https://doi.org/10.1093/cercor/bhad090.
38. Keysers, C., Gazzola, V., and Wagenmakers, E.-J. (2020). Using Bayes factor hypothesis testing in neuroscience to establish evidence of absence. Nat. Neurosci. *23*, 788–799. https://doi.org/10.1038/s41593-020-0660-4.

STAR★METHODS

KEY RESOURCES TABLE

REAGENT or RESOURCE	SOURCE	IDENTIFIER
Deposited data		
Data	https://etsin.fairdata.fi	Etsin Data: https://doi.org/10.23729/fd-fde5397b-d01f-368a-9be1-a750d5f4d589
Experimental models: Organisms/strains		
Rat (male, Lister-hooded, out-bred)	Charles River (Germany)	
Software and algorithms		
Code	https://etsin.fairdata.fi/	Etsin Code: https://doi.org/10.23729/fd-fde5397b-d01f-368a-9be1-a750d5f4d589
JASP (Bayesian statistical analysis)	https://jasp-stats.org/	Version 0.19 (Intel)
Other		
Multi-electrode probes	Neuronexus A2x32 or Cambridge Neurotech H9x64	

EXPERIMENTAL MODEL AND STUDY PARTICIPANT DETAILS

Male Lister-Hooded rats (140–190 g body weight) were used for single unit recordings ($N = 4$) and pupillometry ($N = 37$). The rats were supplied by Charles River Laboratories (Germany) and were housed in pairs for 7 days prior to implantation of the head-fixation implant. After implantation, rats were single housed on a reversed light-dark (07:00 lights off, 19:00 lights on) cycle. Training and experiments were performed during the rats' active phase. All procedures were carried out after approval by local authorities and in compliance with the German Law for the Protection of Animals in experimental research (Tierschutzversuchstierverordnung) and the European Community Guidelines for the Care and Use of Laboratory Animals (EU Directive 2010/63/EU).

METHOD DETAILS

Surgery

The animal was anesthetized with isoflurane (~1.0–2.0%). Heart rate was monitored throughout surgery. Buprenorphine (0.06 m/kg, s.c.), meloxicam (2.0 mg/kg, s.c.), and enrofloxacin (10.0 mg/kg, s.c.) were administered. An incision was made once the rat was no longer responsive to paw pinch. Skin and connective tissue were removed to expose the skull from the frontal bone to the neck muscle and from left to right temporal muscles. The wound margin was cauterized. The exposed bone was wiped dry and cleaned with 5% hydrogen peroxide. The bone surface was then scratched with a bone curette in a grid pattern to facilitate adhesion of the adhesive for the UV light polymerizing cement used to affix the implant to the skull. Two component UV-curing adhesive (OptiBond, Kerr) was applied to the skull and UV cured for 30 s at full intensity (Superlite 1300, M + W Dental). A custom-made head fixation implant was attached to the skull using UV-curing cement (Tetric EvoFlow, Ivoclar). The dental cement was bonded to the adhesive by UV curing for 60 s at full intensity. In rats that were not implanted with a multi-electrode silcon probe, the chamber was filled with 2-component dental cement (Paladur, Kulzer). In cases where multi-electrode probes were to be implanted, the skull was covered in biocompatible silicone elastomer (KwikCast, WPI) and the implant was closed using a lid and screws. In all rats, the skin was glued to the sides of the implant using tissue glue (Histoacryl, B. Braun).

Rats that were implanted with a multi-electrode silicon probe were first trained in the behavioral task. The rats then underwent a second surgery, in which the lid of the implant and the silicone elastomer was removed. The probe (one rat, A2x32, Neuronexus; two rats, H9x64, Cambridge Neurotech) was implanted into the PFC (target coordinates from bregma: AP: 2.7 mm; ML: 0.8 mm; depth: 3.2–4.4 mm, varying across rats) through a craniotomy. No histological verification of implantation sites was performed and it is thus possible, that recording sites varied slightly across animals. Additionally, a second craniotomy was made over the cerebellum. A reference electrode (99.9% pure silver wire) was inserted through this posterior craniotomy. The craniotomy was filled with viscous, electrically-conductive agar. The open space on the skull was filled with 2-component dental cement (Paladur, Kulzer).

Rats recovered for 5 days after surgery. Buprenorphine (0.06 m/kg, s.c.) was administered every 12 h for 3 days in some rats and other rats were injected with meloxicam (2.0 mg/kg, s.c.) every 24 h for 3 days. Rehydrating and easily consumable food was provided (DietGel Recovery, ClearH2O).

Handling and water restriction

For five days prior to surgery, the rats were handled twice a day, once in the morning and in the evening. Each session lasted at least 5 min. After five days of post-surgical recovery, access to water was restricted. During training and experiments, the rats were given 8-12 mL total water per day. Most of the water was consumed as reward during the behavioral task. The remainder of the total water volume was supplied to the rats in the cage after training. The total volume of water available daily was restricted to this level for between 5 and 14 days, while rats learned and performed stimulus discrimination experiments. After an epoch of restricted water availability, rats were provided *ad libitum* access to water for 24 h.

Head-fixation and behavioral apparatus

The rat was head-fixed on a cylindrical, non-motorized fibreglass treadmill that rotated forward or backward freely on low-friction ball bearings. The treadmill and head-fixation apparatus were inside a large Faraday cage (approximately 2 m $\times$ 2 m x 2 m) with sound proofing material. A TTL pulse-controlled pump was used to deliver 10% sucrose water via a reward port that was placed at the mouth of the rat. A computer screen (behind glass with electromagnetic shielding designed to not cause a Moire effect) in front of the rat was used to display visual stimuli covering the entire visual field of the rat. Treadmill angular position was recorded via an analog signal output from a rotary encoder (MA3-A10-125-B, US Digital) attached to the rotational axis of the cylindrical treadmill. The signal output varied between 0 V and +5 V, which mapped linearly to the rotational angle of the treadmill. The signal was sampled at 32 kHz, digitized (Neuralynx signal acquisition system), and velocity was calculated offline (in MATLAB). Video for pupillometry was recorded from the right eye at 45 fps under near-infrared illumination (M850L3, Thor Labs LED, with COP4-B, Thor Labs collimation optics). Frames were recorded with a near-infrared camera (G-046B, Allied Vision) and a variable zoom lens, fixed 3.3x zoom lens, and 0.25x zoom lens attached in-line (1–60135, 1–62831, 6044, Polytec). The camera provided a TTL pulse with each video frame, which was recorded by the Neuralynx signal acquisition system at 32 kHz.

Habituation to head-fixation and behavioral task training

Habituation to head-fixation consisted of a single 20 min session. After habituation, rats were trained to commit an instrumental response for reward. Approximately 5 μL of reward solution (10% sucrose in water) was delivered for small "shaking" or body movements on the treadmill. The threshold for triggered reward was gradually increased to train the rat to make larger body movements and eventually steps. Threshold crossings were marked with a bridging stimulus (0.1 s duration, 500 Hz auditory tone) to aid in learning the link between movement and reward. Eventually, rats would continuously walk and receive reward. This stage required from 3 to 10 sessions (one per day). Once an animal was running and licking simultaneously (which yielded approximately 7 mL of reward solution in a session lasting 20–30 min), we trained the rat to make instrumental (Go) responses contingent upon the presentation of a visual stimulus.

Initially, we presented a 15 s duration visual stimulus. The stimulus was a full field, black and white drifting grating (2.4 cycles/sec, 0.005 cycles/pixel spatial frequency, 75 deg orientation). Rats were trained to respond to the stimulus by continuously delivering reward for running during stimulus presentation. Reward delivery was triggered by crossing a threshold (a.u.) that was the same for all rats and all sessions and set at a level that was associated with bilateral locomotion. The stimulus was followed by an intertrial interval (ITI). The ITI duration was drawn randomly from a distribution ranging from 2 to 3 s (0.05 s bins size).

After 2 sessions, the rats were trained to not respond prior to stimulus onset. The ITI was reduced to 1 to 2 s, and any running that crossed a velocity threshold (manually set to capture running, same for all rats and sessions) resulted in a 0.5 s time-out from the task and a resetting of the ITI. After one or two sessions, the rats started to suppress running during the ITI. Once this was achieved, we reduced stimulus duration in small steps (10 s, 5 s, 2.5 s) over a few sessions. When stimulus duration is 2.5 s, rats exhibit a vigorous and low-latency response upon stimulus onset. At this point in training, we reduce the ITI to 0.5 to 1 s and, after a few sessions, we reduce stimulus duration to 1.5 s (i.e., a speeded reaction time task). Rats were given 600 trials per session. This typically yielded approximately 6 mL of sucrose solution during the task. Behavior was considered stable when omission rate was below 10%.

The Go/NoGo paradigm was introduced with the addition of a NoGo stimulus. The NoGo stimulus was at least 70° different from the Go stimulus. Go and NoGo stimulus trials were delivered in pseudo-random order and in equal proportion. At most, two trials of the same stimulus type could occur consecutively. A Go response required crossing a distance threshold, which roughly corresponded to taking one step. A response offset window (0–0.75 s after stimulus onset) was introduced to compensate for the prepotent drive to respond. During this period, running did not count toward the distance threshold. This allowed low latency movements but forced the rat to appraise the stimulus and make a decision. After the offset window, crossing the distance threshold caused the stimulus to disappear. Hits were rewarded (three 7 μL pulses). Responses to the NoGo stimulus led to an auditory error signal (0.5 s duration, brown noise, 60 dB) and a time-out of 6 s prior to the next ITI. Training was complete when performance was above 85% and omission rate was less than 10%.

Neurophysiological recordings and spike sorting

Wideband (0.1 Hz–10 kHz) signals were recorded at 32 kHz (Digital Lynx SX, Neuralynx). Automatic spike sorting was performed using KiloSort 4.0.[36] Afterward, the outputs were manually curated using standard criteria (i.e., stable firing rate, waveform similarity, auto- and cross-correlograms).

QUANTIFICATION AND STATISTICAL ANALYSIS

Single unit spike count analysis

A Go stimulus-preferring unit responded to the Go stimulus and not to the NoGo stimulus on "pure" Correct Rejection trials, which had little-to-no running. Spike count peri-stimulus time histograms (0.1 s bin size, −0.5 s–1.5 s window around stimulus onset) were z-scored to the trial-averaged spike counts in the 0.5 s before stimulus onset for each unit. The unit was considered responsive to the stimulus, if the Z score was greater than 2 for three consecutive bins in the post-stimulus window (0–0.3 s). We quantified the peak activity of units as the maximal z-scored spike count in the peri-stimulus time histogram. The Hit/Omission index was calculated as:

$$\frac{Peak_{Hit} - Peak_{Omission}}{Peak_{Hit} + Peak_{Omission}}$$

ITI analysis

Transitions from stationary to running during the inter-trial interval were detected by identifying velocity peaks larger than 1 a.u. and with no other peaks present in the 0.4 s directly prior to the peak. A total of 1,297 such take-off events were identified. These events came from sessions in which 47 of the 58 Go stimulus-preferring units were recorded. For the sessions in which the remaining 11 units were recorded we could not find take-off events during the ITI. Take-off time was assigned to the moment when the velocity crossed a threshold of 0.25. The same threshold was applied for alignment of Hit trial velocity and neuronal activity to take-off.

Pupil analysis

Pupillometry was implemented using a custom computer vision algorithm built with the openCV package in Python 3.7. A detailed description of the method is in our prior work.[37]

Statistics

This study used 40 male Lister-Hooded rats (3 for single unit recordings and 37 for pupillometry). Bayesian statistics (JASP software) were used to assess evidence in favor of the null hypothesis and in favor of the alternative hypothesis.[38] We report BF10 which reports the evidence in favor of the alternative hypothesis over evidence favoring the null hypothesis. All analyses used a one-way ANOVA. The single unit activity data in Figure 3A were analyzed with a repeated-measures ANOVA because the same single units were compared across 3 conditions. The trialwise velocity data in Figure 4C were analyzed with an independent samples ANOVA because there were different trial numbers within the 3 conditions (small, medium, and large pupil size) that were being compared. This is due to pupil size freely varying across sessions and rats. We also report traditional ANOVA results with p-values alongside Bayesian statistics and Bonferroni-corrected p-values for post-hoc t-tests. Due to a lack of normality, the trialwise velocity data in Figure 4C were additionally analyzed with a Kruskal-Wallis test and post-hoc Dunn test after log-transformation of the data.